# A role for Rab14 in the endocytic trafficking of GLUT4 in 3T3-L1 adipocytes

**Sam E. Reed[1,*], Lorna R. Hodgson[1,*], Shuang Song[1,‡], Margaret T. May[2], Eoin E. Kelly[3], Mary W. McCaffrey[3], Cynthia C. Mastick[4], Paul Verkade[1] and Jeremy M. Tavaré[1,§]**

[1]School of Biochemistry, University of Bristol, Bristol BS8 1TD, UK
[2]School of Social and Community Medicine, University of Bristol, Bristol BS8 2PS, UK
[3]Molecular Cell Biology Laboratory, Department of Biochemistry, Biosciences Institute, University College Cork, Cork, Ireland
[4]Department of Biochemistry and Molecular Biology, University of Nevada, 1664 North Virginia Street, Reno, NV 89557, USA

*These authors contributed equally to this work
‡Present address: The School of Medicine, King's College London, Franklin-Wilkins Building, 150 Stamford Street, London SE1 9NH, UK
§Author for correspondence (j.tavare@bris.ac.uk)

*Accepted 8 February 2013*
*Journal of Cell Science 126, 1931–1941*

*doi: 10.1242/jcs.104307*

## Summary

Insulin enhances the uptake of glucose into adipocytes and muscle cells by promoting the redistribution of the glucose transporter isoform 4 (GLUT4) from intracellular compartments to the cell surface. Rab GTPases regulate the trafficking itinerary of GLUT4 and several have been found on immunopurified GLUT4 vesicles. Specifically, Rab14 has previously been implicated in GLUT4 trafficking in muscle although its role, if any, in adipocytes is poorly understood. Analysis of 3T3-L1 adipocytes using confocal microscopy demonstrated that endogenous GLUT4 and endogenous Rab14 exhibited a partial colocalisation. However, when wild-type Rab14 or a constitutively-active Rab14Q70L mutant were overexpressed in these cells, the colocalisation with both GLUT4 and IRAP became extensive. Interestingly, this colocalisation was restricted to enlarged 'ring-like' vesicular structures (mean diameter 1.3 μm), which were observed in the presence of overexpressed wild-type Rab14 and Rab14Q70L, but not an inactive Rab14S25N mutant. These enlarged vesicles contained markers of early endosomes and were rapidly filled by GLUT4 and transferrin undergoing endocytosis from the plasma membrane. The Rab14Q70L mutant reduced basal and insulin-stimulated cell surface GLUT4 levels, probably by retaining GLUT4 in an insulin-insensitive early endosomal compartment. Furthermore, shRNA-mediated depletion of Rab14 inhibited the transit of GLUT4 through early endosomal compartments towards vesicles and tubules in the perinuclear region. Given the previously reported role of Rab14 in trafficking between endosomes and the Golgi complex, we propose that the primary role of Rab14 in GLUT4 trafficking is to control the transit of internalised GLUT4 from early endosomes into the Golgi complex, rather than direct GLUT4 translocation to the plasma membrane.

**Key words:** Adipocyte, GLUT4, Insulin, Intracellular trafficking, Rab14

## Introduction

Insulin enhances the uptake of glucose into adipocytes and muscle cells by promoting the redistribution of the glucose transporter isoform 4 (GLUT4) from intracellular compartments to the cell surface (Huang and Czech, 2007; Larance et al., 2008; Leney and Tavaré, 2009). In basal adipocytes, the majority of GLUT4 is sequestered in tubulo-vesicular structures including recycling endosomes, the *trans*-Golgi Network (TGN), and in a discrete population of vesicles called GLUT4 storage vesicles (GSVs). The predominant effect of insulin is to deliver GLUT4 in the GSVs to the cell surface, although it also increases the cycling of GLUT4 through endosomes to the cell surface (Welsh et al., 2005).

Insulin redistributes GLUT4 by activating the protein kinase, AKT2 (protein kinase Bβ), which in turn phosphorylates AKT substrate of 160 kDa (AS160/TBC1D4) (Sakamoto and Holman, 2008). AS160 is a Rab GTPase activating protein (Rab GAP) (Kane et al., 2002), which is present on immunopurified GLUT4 vesicles from basal adipocytes (Larance et al., 2005; Mîinea et al., 2005). AS160 has been implicated as a negative regulator of insulin-stimulated GLUT4 delivery to the cell surface in the basal state by maintaining particular RabGTPases in the GDP-bound (inactive) state using its GAP domain (Eguez et al., 2005; Larance et al., 2005; Sano et al., 2003). Upon insulin stimulation, phosphorylation of AS160 is proposed to promote its dissociation from GLUT4 vesicles (Kane et al., 2002; Larance et al., 2005) and/or inhibit its GAP activity (Stöckli et al., 2008), which in turn permits the target RabGTPases to enter the GTP-bound (active) state and thus stimulate the delivery of GLUT4 to the cell surface.

RabGTPases regulate a plethora of vesicle trafficking events including vesicle formation, vesicle movement and vesicle attachment to its target membrane (Zerial and McBride, 2001). While multiple Rabs have been proposed to be targets for AS160, the physiologically relevant Rab targets for GLUT4 trafficking are still being debated (Ishikura et al., 2008; Kaddai et al., 2008; Sakamoto and Holman, 2008). It has been shown that Rabs including 2A, 8A, 10 and 14 are effective substrates for a recombinant GAP domain of AS160 *in vitro* (Mîinea et al., 2005), and that Rabs 10, 11A, 11B and 14 are found on immuno-isolated GLUT4 vesicles from 3T3-L1 adipocytes (Larance et al., 2005). Rab10 has been proposed to be a target for AS160 in 3T3-L1

adipocytes as the small increase in cell surface GLUT4 in non-insulin-stimulated cells observed as a result of siRNA-mediated knockdown of AS160, was partially inhibited by ablating Rab10 (Sano et al., 2007). Rabs 8A, 13 and 14 have been proposed to be targets for AS160 in L6 muscle cells as the inhibition of insulin-stimulated GLUT4 delivery to the cell surface arising from expression of non-phosphorylatable AS160 is relieved when these Rabs are co-expressed (Ishikura et al., 2007; Sun et al., 2010). Rab11 has been proposed to be involved in the endocytic trafficking of GLUT4 in cardiac muscle (Kessler et al., 2000; Schwenk et al., 2007; Uhlig et al., 2005) and 3T3-L1 adipocytes (Zeigerer et al., 2002), and more specifically in regulating the transport of GLUT4 from endosomes into GSVs in the case of the latter. Similarly, Rab4 has been proposed to mediate the endocytic sorting of GLUT4 into GSVs in 3T3-L1 adipocytes (Mari et al., 2006). Finally, Rab31 (also known as Rab22B) has been implicated in insulin-stimulated GLUT4 delivery to the cell surface in 3T3-L1 adipocytes, but the trafficking step affected remains unclear (Lodhi et al., 2007). Whether Rabs 4, 11 and 31 regulate GLUT4 trafficking independently of AS160 *in vivo* is currently unclear.

The intracellular site of action of Rab14 on GLUT4 trafficking is poorly understood, particularly in adipocytes. Here we show that unlike other Rabs commonly found on GLUT4 vesicles, Rab14, when overexpressed, extensively colocalised with GLUT4 in enlarged endosomal vesicular structures. Characterisation of the nature of this compartment leads us to suggest that the primary role for Rab14 is to control the transit of endocytosing GLUT4 through early endosomes towards the TGN, rather than in the direct translocation of GSVs to the plasma membrane.

## Results

### GLUT4 and endogenous Rab14 colocalise in 3T3-L1 adipocytes

We first examined whether endogenous GLUT4 and endogenous Rab14 colocalised in 3T3-L1 adipocytes using confocal microscopy with specific antibodies raised against these proteins. GLUT4 and Rab14 were both found within the complex arrangement of membranes found in the perinuclear region, however at this level of resolution we could not confirm that this represented colocalisation within the same tubulo-vesicular structures. When we looked at the more dispersed peripheral vesicles, there was evidence for colocalisation but only in a relatively small number of structures (Fig. 1A). These observations are similar to a previous report from James and co-workers (Larance et al., 2005). To examine the apparent colocalisation further we co-expressed mCherry-tagged Rab14 with GFP-tagged GLUT4. In contrast to the situation with the

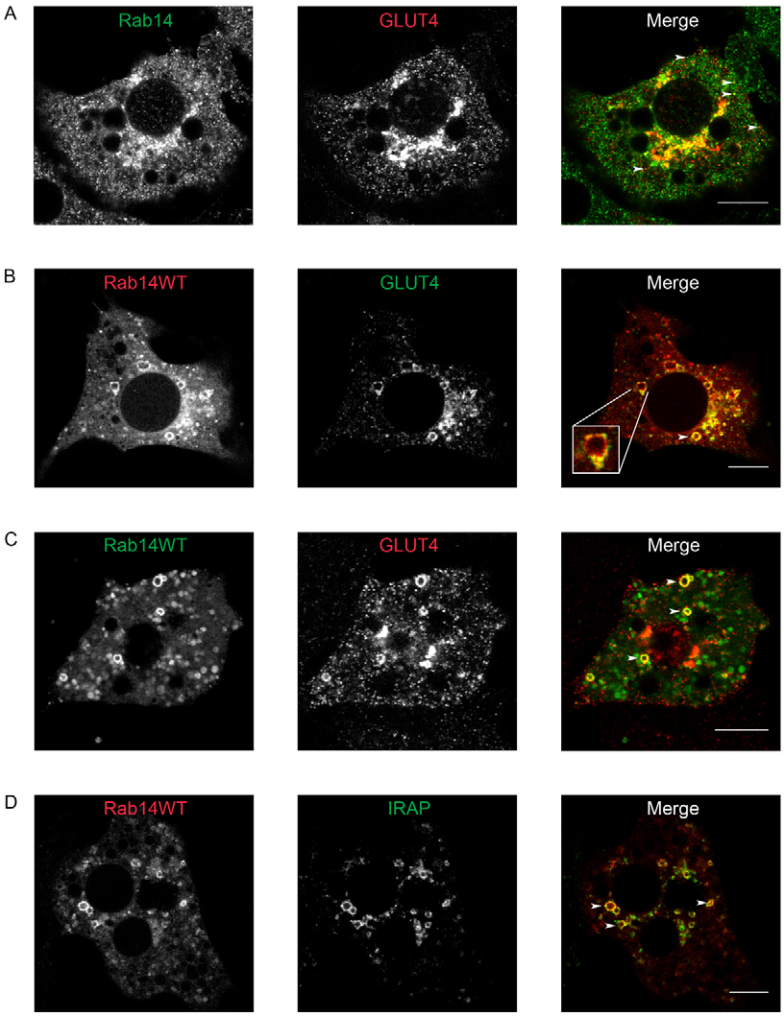


**Fig. 1. Rab14 gives rise to enlarged vesicular structures containing Rab and GLUT4.** (**A**) 3T3-L1 adipocytes were serum starved for 3 hours, fixed, permeabilised and stained with antibodies against Rab14 and GLUT4. White arrowheads indicate puncta positive for Rab14 and GLUT4. (**B**) 3T3-L1 adipocytes were electroporated with plasmids encoding HA-GLUT4-GFP and mCherry-Rab14WT. After 24 hours, cells were serum starved for 3 hours and fixed. (**C**) 3T3-L1 adipocytes were electroporated with a plasmid encoding GFP-Rab14WT. After 24 hours, cells were serum starved for 3 hours, fixed, permeabilised, and stained with an antibody against GLUT4. (**D**) 3T3-L1 adipocytes were electroporated with plasmids encoding mCherry-Rab14WT and IRAP-GFP. After 24 hours, cells were serum starved for 3 hours and fixed. All cells were imaged by confocal microscopy. White arrowheads indicate enlarged vesicular structures positive for Rab14 and either GLUT4 or IRAP. Scale bars: 10 µm.

endogenous proteins, we found extensive colocalisation between the two overexpressed proteins (Fig. 1B). However, importantly, this colocalisation was most pronounced on enlarged vesicular structures that often possessed a visible lumen and which were located throughout the cell, frequently in clusters. They varied in diameter from ~1 to 3 μm, and were found in ~70% of cells that expressed mCherry-Rab14. On closer inspection, while the entire vesicle perimeter was positive for mCherry-Rab14, the GLUT4-GFP distribution was typically discontinuous and appeared to occur in subregions of the vesicle (e.g. inset in Fig. 1B). The enlarged vesicular structures were also positive for endogenous GLUT4 (Fig. 1C) and an overexpressed GFP-tagged insulin-responsive aminopeptidase (IRAP-GFP; Fig. 1D) that is well established to traffic in a similar manner to GLUT4 (Ross et al., 1997; Ross et al., 1996).

### The formation of enlarged vesicles is specific to overexpressed Rab14

To assess the specificity of this effect, we examined whether the overexpression of other Rabs produced a similar phenotype. We initially examined mCherry-tagged versions of Rabs 8A, 10, 11A, 14 and 31 as these had previously been demonstrated to be either: (i) a substrate for the AS160 RabGAP or (ii) associated with purified GLUT4 vesicle preparations. Colocalisation of these proteins was assessed in both basal and insulin-stimulated cells. In basal cells, all Rabs showed some apparent colocalisation with GLUT4 in the perinuclear region and occasionally in some small more peripheral puncta (supplementary material Fig. S1). Insulin treatment did not appear to have any influence on the extent of colocalisation, as none of the Rabs translocated to the plasma membrane, and no loss of GLUT4 from cytoplasmic vesicles was observed accompanying GLUT4 translocation (data not shown). Thus mCherry-Rab14 was unique among the Rabs we initially examined in inducing the formation of enlarged vesicular structures in 3T3-L1 adipocytes.

We next examined whether this phenotype was also observed in the presence of mutant forms of Rabs which are either in a GTP-locked state and so constitutively-active (Q70L in Rab14, or equivalent) via inhibition of GTPase activity, or GDP-locked and dominant-inactive (S25N in Rab14, or equivalent) via an increased binding affinity for GDP than GTP. Constitutively-active mCherry-tagged mutants of Rabs 8A, 10, 11, 14 and 31 or vector alone were co-expressed with GLUT4-GFP and vesicle enlargement was assessed. As with the wild-type forms of these Rabs, enlarged vesicular structures positive for GLUT4-GFP were observed only in the presence of Rab14Q70L (Fig. 2A). In the presence of the Rab14Q70L mutant each adipocyte expressed

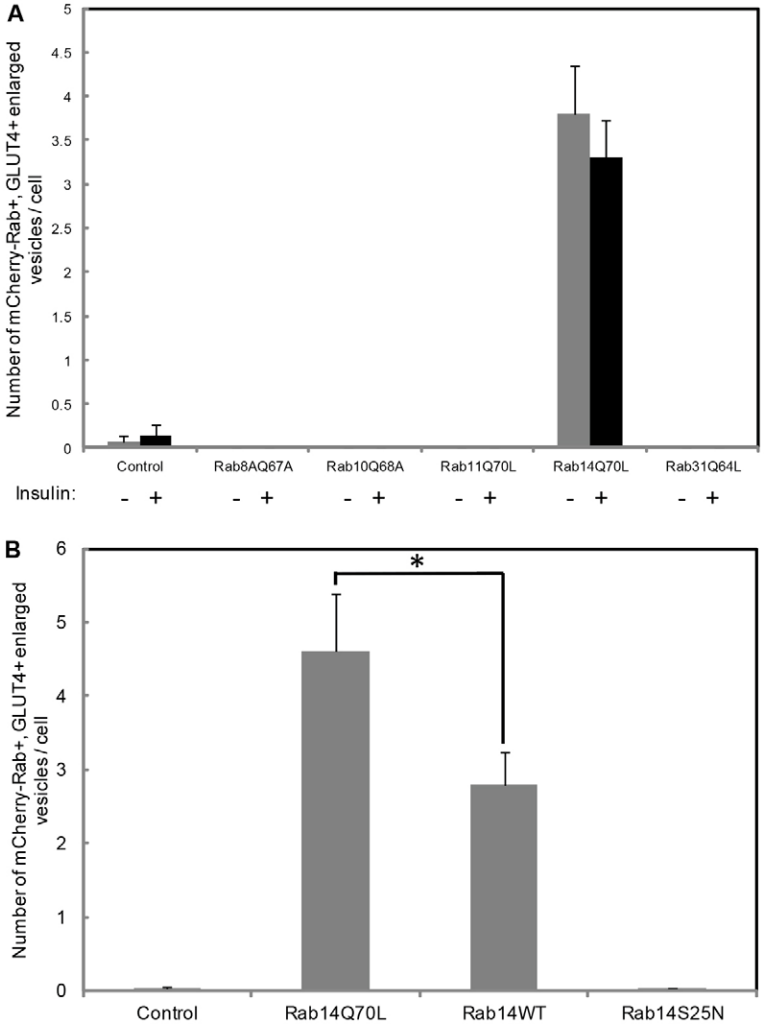


**Fig. 2. Rab14Q70L and Rab14WT, but not Rab14S25N, give rise to enlarged vesicular structures containing Rab14 and GLUT4.** (**A**) 3T3-L1 adipocytes were electroporated with plasmids encoding HA-GLUT4-GFP and either mCherry, mCherry-Rab8AQ67A, mCherry-Rab10Q68A, mCherry-Rab11Q70L, mCherry-Rab14Q70L or mCherry-Rab31Q64L. After 24 hours, cells were serum starved for 3 hours, stimulated for 30 minutes with 87 nM insulin as required, fixed and imaged by confocal microscopy. Shown are the mean number of enlarged vesicular structures positive for Rab and GLUT4 (or in the case of mCherry alone, positive for mCherry and GLUT4) per cell ± s.e.m. from three independent experiments, with 20 cells analysed per experiment. (**B**) 3T3-L1 adipocytes were electroporated with plasmids encoding HA-GLUT4-GFP and either mCherry, mCherry-Rab14Q70L, mCherry-Rab14WT or mCherry-Rab14S25N. After 24 hours, cells were serum starved for 3 hours, fixed and imaged by confocal microscopy. Shown are the mean number of enlarged vesicular structures positive for Rab14 and GLUT4 (or in the case of mCherry alone, positive for mCherry and GLUT4) per cell ± s.e.m. from three independent experiments, with 20 cells analysed per experiment. *$P<0.05$ versus Rab14Q70L.

3.80±0.55 (mean±s.e.m., $n$=3 independent experiments, 20 cells per experiment) enlarged vesicles positive for both the Rab and GLUT4. This number was unaffected by insulin (3.30±0.44). Similarly, insulin had no effect on the diameter of the enlarged vesicular structures (1.35±0.04 μm in basal versus 1.45±0.07 μm in insulin-stimulated cells; mean±s.e.m., $n$=3 independent experiments, 20 cells per experiment).

To explore whether the nucleotide status of Rab14 affected vesicle enlargement, wild-type, constitutively-active and dominant-inactive mCherry-tagged Rab14 mutants, or vector alone, were co-expressed with GLUT4-GFP in 3T3-L1 adipocytes, and vesicle enlargement was assessed. Enlarged structures containing mCherry-Rab14 and GLUT4-GFP were observed in the presence of the constitutively-active and wild-type Rab14, but not the dominant-inactive Rab14S25N mutant (Fig. 2B). The number of enlarged vesicles observed in the presence of the constitutively-active mCherry-Rab14Q70L was significantly greater than in the presence of wild-type mCherry-Rab14 (Fig. 2B), probably reflecting their degree of GTP loading, although the diameters of these structures were the same in each case (1.27±0.05 μm versus 1.24±0.05 μm in the presence of Rab14Q70L and wild-type Rab14, respectively; mean±s.e.m., $n$=3 independent experiments, 20 cells per experiment). Again, insulin had no effect on either the number or diameter of enlarged vesicular structures (data not shown).

### The enlarged vesicular structures contain predominantly early, but also recycling, endosomal markers and are rapidly labelled during endocytosis of GLUT4 and transferrin receptors

To define the nature of the enlarged vesicular structures, constitutively-active Rab14Q70L was expressed in 3T3-L1 adipocytes and its colocalisation with a series of markers of different intracellular compartments was examined. To assess localisation with early endosomes and recycling endosomes, we co-expressed mCherry- or GFP-Rab14Q70L with GFP-2×FYVE of Hepatocyte growth factor-regulated tyrosine kinase substrate (Hrs) and the human transferrin receptor, respectively. The latter was labelled by incubating cells in the presence of fluorescent transferrin for 30 minutes prior to fixation and imaging. As shown in Fig. 3A, there was evidence for very extensive overlap between mCherry-Rab14Q70L and the early endosome marker GFP-2×FYVE/Hrs. The overall degree of colocalisation between mCherry-Rab14Q70L and endocytosed fluorescent transferrin was less than for GFP-2×FYVE/Hrs, although there was clear evidence that the enlarged vesicular structures contained both markers (Fig. 3B). This suggests that the enlarged vesicles which

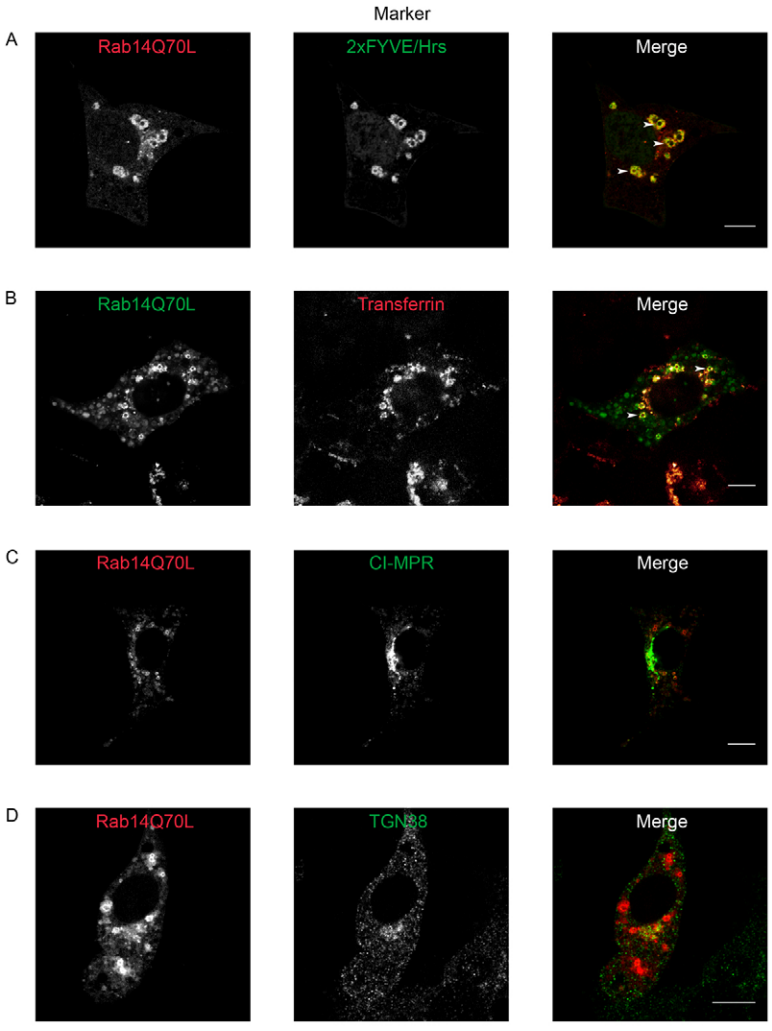


**Fig. 3. Rab14Q70L enlarged vesicular structures contain predominantly early endosomal markers.** (**A**) 3T3-L1 adipocytes were electroporated with plasmids encoding mCherry-Rab14Q70L and GFP-2×FYVE/Hrs. After 24 hours, cells were serum starved for 3 hours and fixed. (**B**) 3T3-L1 adipocytes were electroporated with plasmids encoding GFP-Rab14Q70L and the human transferrin receptor. After 24 hours, cells were serum starved for 3 hours, incubated for 30 minutes with 30 μg/ml transferrin Alexa Fluor 633 and fixed. (**C**) 3T3-L1 adipocytes were electroporated with plasmids encoding mCherry-Rab14Q70L and GFP-CI-MPR. After 24 hours, cells were serum starved for 3 hours and fixed. (**D**) 3T3-L1 adipocytes were electroporated with a plasmid encoding mCherry-Rab14Q70L. After 24 hours, cells were serum starved for 3 hours, fixed, permeabilised and stained with an antibody against TGN38. All cells were imaged by confocal microscopy. White arrowheads indicate enlarged vesicular structures positive for Rab14 and the compartment marker. Scale bars: 10 μm.

contain Rab14Q70L and by inference GLUT4, have characteristics of early and recycling endosomes (although the latter may represent transferrin receptors in transit to the recycling compartment). By contrast there was very little if any convincing overlap between any vesicles containing Rab14Q70L and markers of late endosomes (the cation-independent mannose-6-phosphate receptor; Fig. 3C) or the TGN (TGN38; Fig. 3D).

We next examined the colocalisation of Rab14Q70L with other Rab proteins involved in endocytic trafficking. Almost complete colocalisation was observed between mCherry-Rab14Q70L and GFP-Rab4 in a series of highly enlarged vesicles (Fig. 4A). Significant overlap was also observed between mCherry-Rab14Q70L and GFP-Rab5 (Fig. 4B) although, as shown in the inset to Fig. 4B, this overlap was predominantly restricted to the smaller of the population of enlarged vesicles; the vesicles with the largest diameters being almost completely devoid of Rab5. mCherry-Rab14Q70L showed some overlap with the recycling endosome marker GFP-Rab11 (Fig. 4C) but little or no overlap with the late endosomal marker GFP-Rab7 (Fig. 4D).

To confirm the nature of the enlarged structures comprising Rab14, we used section light electron microscopy. This revealed that GFP-Rab14Q70L was present on the limiting membrane of a compartment that lacked intra-lumenal vesicles strongly suggesting that the vesicles are of early rather than late endosome in origin (Fig. 5). The diameter of the gold-labelled vesicle in Fig. 5B at its widest point is 0.77 μm.

Taken together our data suggest that overexpression of Rab14Q70L, and to a lesser extent Rab14WT, induces a defect in endosomal trafficking such that a build up of membrane occurs in a compartment that has several characteristics of early endosomes. The fact that this compartment could be labelled with fluorescent transferrin suggests that entry of cargo into this pool is dynamic and primarily occurs via endocytosis.

To examine whether GLUT4 also entered the enlarged vesicular structures via endocytosis, we co-transfected adipocytes with mCherry-Rab14Q70L and a haemagglutinin (HA)-tagged GLUT4 fusion protein. In this construct, the HA epitope is in the first exofacial loop of GLUT4 and becomes exposed to the extracellular milieu when GLUT4 is incorporated into the plasma membrane. These adipocytes were incubated in the presence of insulin to promote translocation of HA-GLUT4 to the plasma membrane and then with anti-HA antibody at 15℃ to label surface HA-GLUT4. The cells were warmed to 37℃ and internalisation of the HA-antibody was monitored over time. HA-antibody appeared on the enlarged Rab14Q70L positive vesicles within 10 minutes of raising the temperature (Fig. 6). This observation is consistent with the concept that these structures receive GLUT4 and transferrin receptor (Fig. 3B) cargoes via endocytosis.

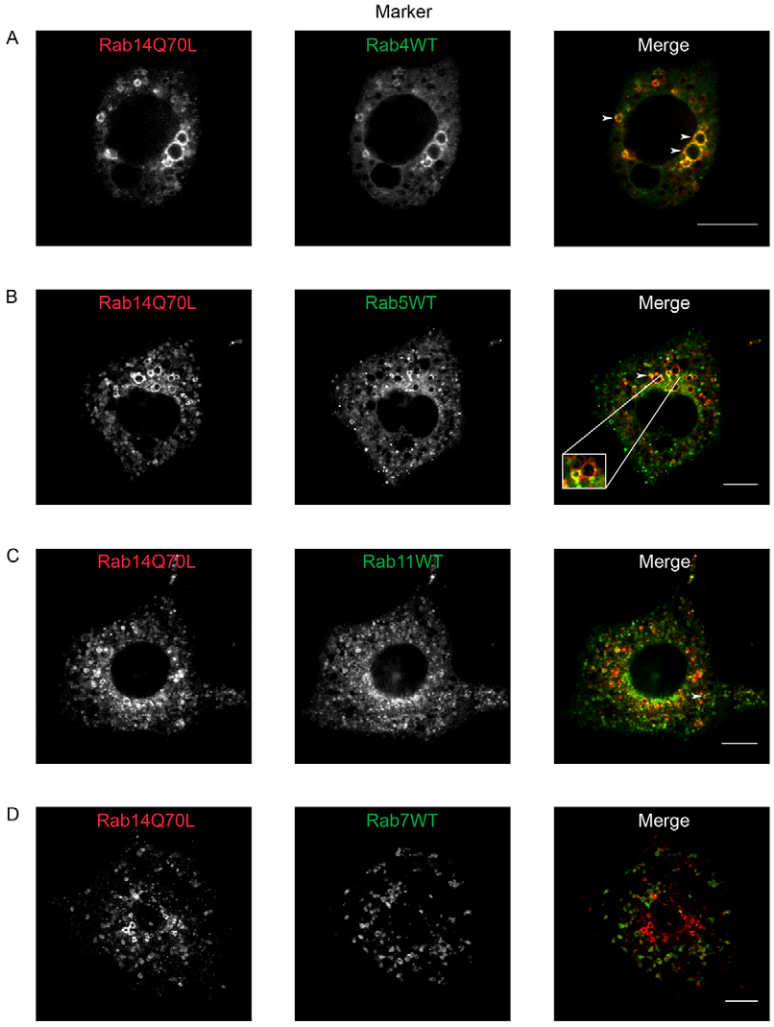


**Fig. 4. Rab14Q70L enlarged vesicular structures contain predominantly early endosomal associated Rabs.** (**A–D**) 3T3-L1 adipocytes were electroporated with plasmids encoding mCherry-Rab14Q70L and GFP-Rabs 4WT, 5WT, 7WT and 11WT. After 24 hours, cells were serum starved for 3 hours, fixed and imaged by confocal microscopy. White arrowheads indicate enlarged vesicular structures positive for Rab14 and the respective Rab. Scale bars: 10 μm.

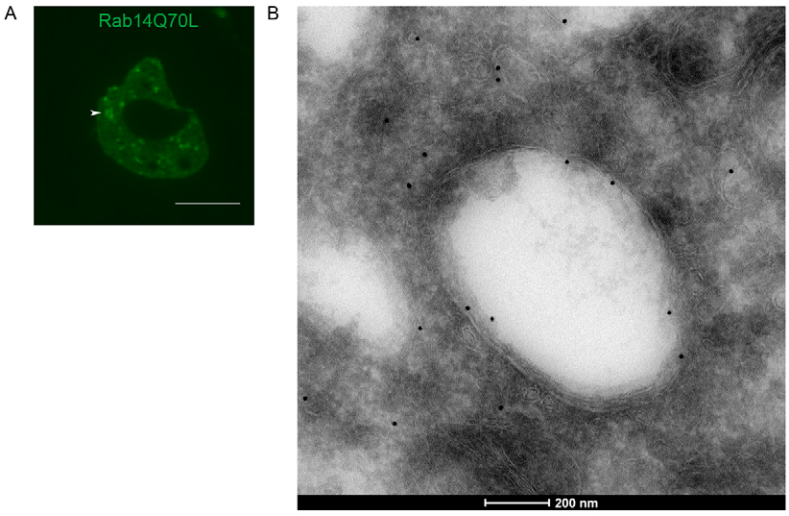


**Fig. 5. Rab14Q70L enlarged vesicular structures contain no intra-lumenal vesicles.** 3T3-L1 adipocytes were electroporated with a plasmid encoding GFP-Rab14Q70L. After 24 hours, cells were serum starved for 3 hours, fixed, embedded in gelatin and copper finder grids prepared, as described in Materials and Methods. (**A**) Rab14 enlarged vesicular structures were identified by widefield fluorescence microscopy. The white arrowhead indicates an enlarged vesicular structure positive for Rab14. Scale bar: 10 μm. (**B**) Grids were labelled with an antibody against GFP and 15 nm gold, and imaged by transmission electron microscopy. Black dots indicate 15 nm gold.

### Rab14Q70L reduces cell surface GLUT4 in the basal and insulin-stimulated states

We next examined the effect of Rab14Q70L on insulin-stimulated GLUT4 translocation to the plasma membrane using the HA-GLUT4-GFP construct. Any GLUT4 that has been fully delivered into the membrane leaflet can be detected by staining fixed non-permeabilised cells for the HA epitope. The GFP at the C-terminus allows for cell surface GLUT4 to be normalised to the total expression of the protein (Welsh et al., 2007). mCherry-Rab14Q70L or mCherry alone were co-expressed with HA-GLUT4-GFP in 3T3-L1 adipocytes, and the presence of GLUT4 at the cell surface was assessed in both basal and insulin-stimulated states. In the presence of mCherry-Rab14Q70L, cell surface GLUT4 in the basal and insulin-stimulated states were reduced to an approximately equivalent degree (52% and 67%, respectively, $n=3$ independent experiments, 20 cells analysed per experiment); indeed the fold-insulin effect was not markedly reduced by the presence of the Rab14Q70L mutant (3.7-fold versus 2.5-fold in control and Rab14Q70L expressing cells) (Fig. 7).

### GLUT4 accumulates in early endosomal compartments in the absence of Rab14

We next examined the effects of shRNA-mediated Rab14 knockdown on the trafficking of GLUT4 through intracellular compartments by following HA antibody uptake from the cell surface. Using confocal microscopy, we could see no apparent difference in the dynamics of HA-antibody uptake through endosomes or other compartments upon Rab14 depletion. We reasoned this may have been due to the low resolving power of light microscopy preventing compartments lying in close juxtaposition from being discriminated from one another. We developed, therefore, a higher resolution quantitative technique employing electron microscopy in which HA-GLUT4 was tagged at the cell surface with gold-labelled anti-HA antibodies at 15℃, and its transit followed from the plasma membrane into a series of morphologically distinct intracellular compartments by warming the cells to 37℃ (supplementary material Fig. S2). Time course experiments demonstrated that labelling of early endosomal compartments was relatively rapid, peaking at 30 minutes before declining thereafter, whereas the entry of gold-labelled anti-HA antibodies into late endosomes, lysosomes and compartments close to the nucleus was slower (supplementary material Fig. S3).

3T3-L1 adipocytes were stably transfected with lentiviral constructs expressing either scrambled or Rab14 shRNAs and then western blotted to confirm the knockdown of Rab14 (Fig. 8A). We next incubated these cells with gold-labelled anti-HA antibodies at 15℃ and allowed endocytosis at 37℃ to proceed for 60 minutes before fixing the cells and quantitatively analysing for the distribution of gold among the morphological compartments defined in supplementary material Fig. S2. As shown in Fig. 8, Rab14 knockdown resulted in the accumulation of GLUT4 in plasma membrane localised vesicles/tubules and in early endosomes with 4 or fewer intra-lumenal vesicles, in parallel with a concomitant reduction in GLUT4 in early endosomes with 5–8 intralumenal vesicles or small vesicles (50–100 nm in diameter) which clustered together in the perinuclear region (Fig. 8). There was a trend for a reduction of gold accumulation in lysosomes and tubular–vesicular

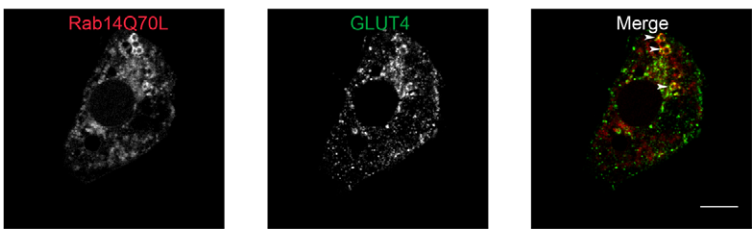


**Fig. 6. Rab14Q70L enlarged vesicular structures are accessible to internalised GLUT4.** 3T3-L1 adipocytes were electroporated with plasmids encoding HA-GLUT4 and mCherry-Rab14Q70L. After 24 hours, cells were serum starved for 3 hours, stimulated for 30 minutes with 87 nM insulin, incubated with an antibody against the HA epitope for 30 minutes at 15℃ and incubated at 37℃ for 10 minutes prior to fixation. Fixed cells were permeabilised and HA visualised using a fluorescently labelled secondary antibody. White arrowheads indicate enlarged vesicular structures positive for Rab14 and internalised GLUT4. Scale bar: 10 μm.

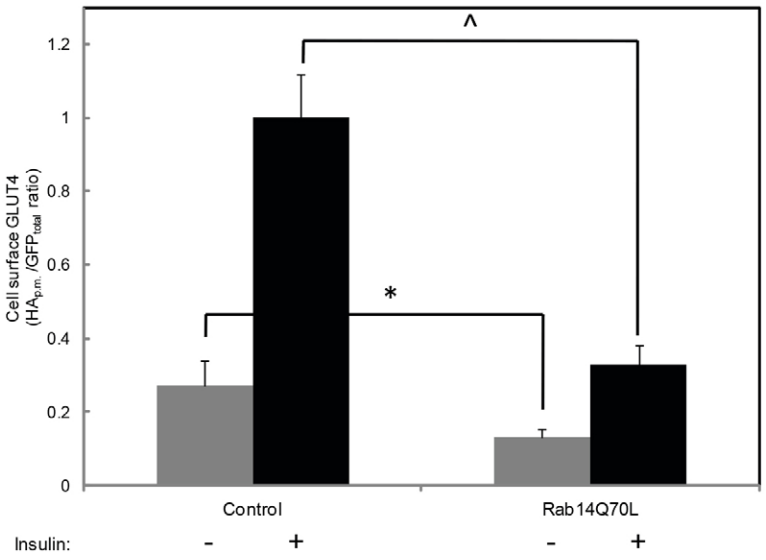


**Fig. 7. Rab14Q70L reduces cell surface GLUT4 in the basal and insulin-stimulated states.** 3T3-L1 adipocytes were electroporated with plasmids encoding HA-GLUT4-GFP and either mCherry or mCherry-Rab14Q70L. After 24 hours, cells were serum starved for 3 hours, stimulated for 30 minutes with 87 nM insulin, as required, and fixed. Fixed, non-permeabilised cells were stained with an antibody against the HA epitope to detect cell surface GLUT4. Cells were imaged and GLUT4 translocation measured as described in Materials and Methods. Shown are the mean amounts of cell surface GLUT4 ± s.e.m. from three independent experiments, with 20 cells analysed per experiment. The values in each experiment have been normalised to a value of 1 for the control with insulin. *$P<0.05$ versus control basal, $^{\wedge}P<0.05$ versus control insulin.

compartments near the nucleus, although these did not reach significance (Fig. 8). The data support a role for Rab14 in the trafficking of GLUT4 through early endosomal compartments, in particular as they begin to accumulate more than four intralumenal vesicles.

## GLUT4 vesicles fusing with the plasma membrane lack Rab14

To determine if Rab14 may play a role in the exocytosis of GLUT4, we used total internal reflection fluorescence (TIRF) microscopy to determine if Rab14 is on GLUT4 vesicles

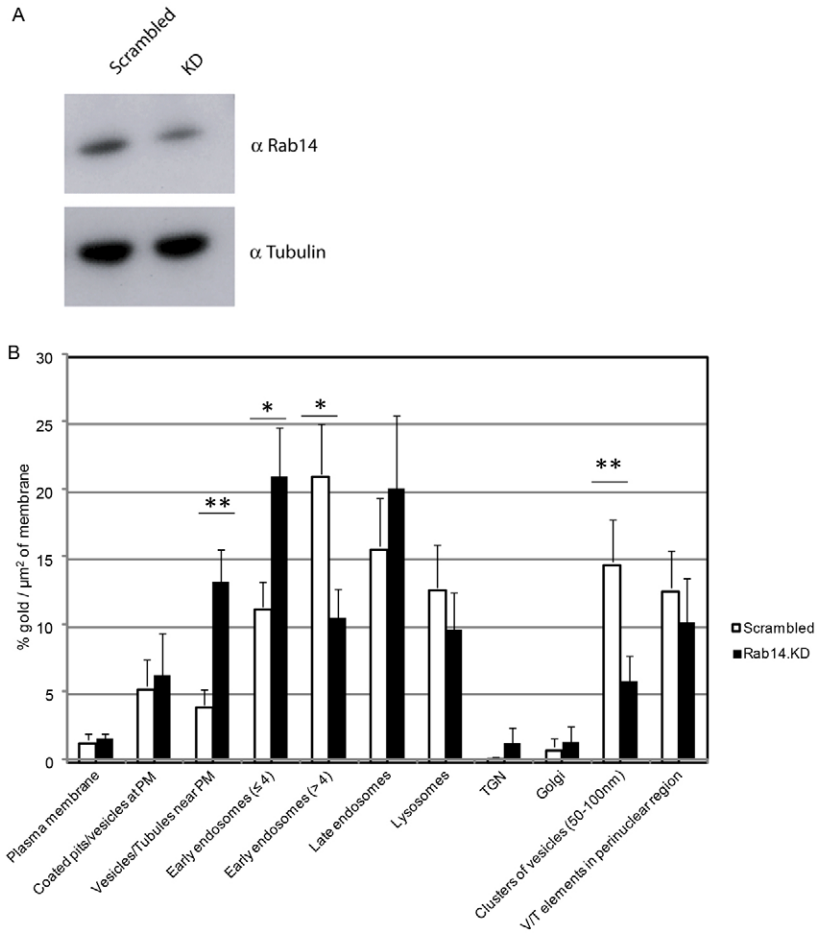


**Fig. 8. GLUT4 collects in early endocytic compartments in the absence of Rab14.** (**A**) Lysates of either Rab14 knockdown or scrambled 3T3-L1 adipocytes were immunoblotted for Rab14 or α tubulin (loading control). (**B**) Rab14 knockdown or scrambled 3T3-L1 adipocytes expressing HA-GLUT4-GFP were serum starved for 3 hours and stimulated for 20 minutes with 87 nM insulin. Cells were incubated with anti-HA antibody, rabbit anti-mouse bridging antibody and 5 nm Protein A gold for 20 minutes at 15℃. Cells were warmed to 37℃ for 60 minutes before fixation, processing for transmission electron microscopy and quantification, as described in Materials and Methods. The graph represents the amount of gold in each compartment as a percentage of total gold (mean ± s.e.m.; *$P<0.05$ or **$P<0.01$ by Kruskal–Wallis ANOVA). Data are derived from two independent experiments with 11 and 9 scrambled and Rab14 knockdown cells analysed, respectively.

undergoing fusion with the plasma membrane in response to insulin. mCherry-Rab14WT or HA-GLUT4-mCherry were co-expressed with IRAP-pHluorin [a well characterised GLUT4 vesicle resident protein (Jiang et al., 2008)] in 3T3-L1 adipocytes, and the IRAP-pHluorin vesicles fusing with the plasma membrane in the insulin-stimulated state were analysed to determine if they were positive for mCherry-Rab14WT immediately prior to fusion. pHluorin is a pH-sensitive GFP mutant, the fluorescence of which increases substantially at a pH greater than 6 (Jiang et al., 2008). Thus in cells maintained in medium at physiological pH (7.2), IRAP-pHluorin vesicle fluorescence increases (flashes) upon fusion with the plasma membrane, subsequent to which the fluorescence diffuses outwards as the transporter moves laterally in the membrane (supplementary material Fig. S4). Rab14WT was found on 3.3%±2.8 of IRAP-pHluorin vesicles (mean±s.e.m., $n=217$ vesicles from 5 cells from 3 independent experiments), a value which is lower than the ~40% reported by Chen and co-workers (Chen et al., 2012). In contrast, HA-GLUT4-mCherry was found on 56.5%±5.2 of IRAP-pHluorin vesicles (mean±s.e.m., $n=217$ vesicles from 4 cells from 3 independent experiments). Our finding is more consistent with a role for Rab14 in the trafficking of GLUT4 through endosomes rather than fusion of GLUT4 vesicles with the plasma membrane.

## Discussion

Several lines of evidence point towards a role for Rab14 in GLUT4 trafficking. This includes the facts that Rab14 is present in purified adipocyte GLUT4 vesicle preparations (Larance et al., 2005), that Rab14 is a substrate, at least *in vitro*, for the AS160 RabGAP (Mîinea et al., 2005) and that siRNA-mediated knockdown of Rab14 inhibits insulin-stimulated GLUT4 translocation to the plasma membrane of muscle cells (Ishikura and Klip, 2008). Despite these important observations, the precise intracellular compartment at which Rab14 influences GLUT4 trafficking is not known. The effect of Rab14 knockdown in L6 cells is suggestive of an action on GLUT4 translocation from the GSV compartment to the plasma membrane, however evidence in other cell types suggests that Rab14 is more relevant for cargo trafficking between endosomes and the TGN. We utilised a series of Rab14 constructs to explore this apparent paradox.

In our studies we found that overexpression of wild-type Rab14 in 3T3-L1 adipocytes gave rise to an enlargement, or swelling, of a Rab14-positive compartment containing GLUT4 and IRAP (Fig. 1). We further showed that this swollen phenotype was observed in the presence of a GTP-locked Rab14 mutant (Rab14Q70L; Fig. 2A) but not when using an inactive GDP-loaded Rab14 mutant (Rab14S25N; Fig. 2B). Several factors suggested that the enlarged vesicles were early endosomal in nature including the presence of markers of early endosomes (2×FYVE/Hrs, Rab4 and Rab5; Figs 3, 4), the lack of intra-lumenal vesicles more characteristic of late endosomes (Fig. 5) and the rapid entry into this compartment of GLUT4 and transferrin receptors undergoing endocytosis from the plasma membrane (Fig. 3B; Fig. 6).

Rab14 has been found on endosomes and Golgi membranes in several cell types (Junutula et al., 2004; Proikas-Cezanne et al., 2006). Subsequent work localised the protein predominantly to the early/recycling endosomal pathway (Kelly, et al., 2009). More recently, Rab14 has been reported to localise to an intermediate compartment of the transferrin receptor recycling pathway prior to Rab11 but after compartments positive for Rab4 and Rab5 (Linford et al., 2012). Furthermore, the overexpression of Rab14Q70L has been reported to induce the enlargement of an early endosomal compartment in normal rat kidney cells resulting in a defect in trafficking cargo (transferrin) out of early endosomes and into the TGN (Junutula et al., 2004). The endocytosis and sorting of GLUT4 has been proposed to involve a transit from early endosomes through to the TGN (Martin et al., 2000; Shewan et al., 2003; Slot et al., 1991a; Slot et al., 1991b) thus, in adipocytes Rab14Q70L could promote swelling of the GLUT4 containing early endocytic compartment by inhibiting the fission and sorting of GLUT4 vesicles out of early endosomes en route to the TGN and from there into GSVs.

Alternatively, Rab14Q70L could promote a swelling of the GLUT4 containing early endocytic compartment via an increased rate of fusion of vesicles undergoing endocytosis from the plasma membrane, a hypothesis that is very difficult to test using existing tools. Interestingly, however, we did notice that some particularly large and swollen Rab14Q70L-positive vesicles were essentially devoid of Rab5, but were surrounded by smaller swollen vesicles positive for both Rab5 and Rab14 (as shown in the inset to Fig. 4B). Rab5 is well established to play an important role in the docking of clathrin-coated endocytic vesicles with early endosomes (Bucci et al., 1992; Stenmark et al., 1994) and GLUT4 is known to endocytose at least in part via a clathrin-mediated mechanism (Antonescu et al., 2008). The smaller Rab5/Rab14 positive vesicles could represent endocytic vesicles in the process of undergoing fusion to form the larger Rab14 positive vesicles, a process immediately followed by the release of Rab5. This would be consistent with the proposed role for Rab14 in the fusion of phagosomes with endosomes in macrophages and *Dictyostelium* (Harris and Cardelli, 2002; Kyei et al., 2006).

When we examined insulin-regulatable GLUT4 translocation, we found that the Rab14Q70L mutant reduced both basal and insulin-stimulated GLUT4 translocation to the plasma membrane by approx. 50% (Fig. 7), without altering the fold-effect of insulin itself (approx. 3-fold). In 3T3-L1 adipocytes, GLUT4 continuously recycles between the plasma membrane and intracellular compartments, even in the basal state (Karylowski et al., 2004). During this dynamic recycling any endocytosed GLUT4 would likely accumulate in the early endocytic compartment sequestering GLUT4 within early endosomes and away from the insulin-responsive GSV compartment thus lowering basal and insulin-stimulated translocation. Knockdown of Rab14 in 3T3-L1 adipocytes inhibited the transit of GLUT4 through early endosomes (Fig. 8) suggesting that the mechanism by which Rab14Q70L causes a swelling of the GLUT4 containing early endosomal compartment, involves an inhibition of cargo flux through early endosomes rather than by inhibiting the direct translocation of GLUT4 from GSVs to the plasma membrane per se. This is consistent with our observation using TIRF microscopy that the majority of IRAP vesicles fusing with the plasma membrane in response to insulin are devoid of Rab14 (supplementary material Fig. S4).

In rat adipocytes overexpression of Rab4 has also been reported to reduce basal and insulin-stimulated cell surface GLUT4myc levels (Cormont et al., 1996), although the mechanism underlying the effect was not established. Interestingly, overexpression of wild-type Rab4 also induces

the formation of enlarged early endosomes, but only in the presence of the Rab4-interacting protein Rabip4 (Mari et al., 2006) (also known as RUFY1; Yamamoto et al., 2010). In our hands the magnitude of the effect of Rab4 overexpression was very similar to that observed with Rab14 but apparently independent of the requirement for co-expression of Rabip4/RUFY1 (supplementary material Table S1). Rab4 and Rab14 exhibit a high degree of colocalisation (Fig. 4A), are highly related at the amino acid sequence level (Pereira-Leal and Seabra, 2000) and both bind to Rabip4/RUFY1 (Yamamoto et al., 2010). This suggests that Rabs 4 and 14 may be functionally redundant, however it should be noted that Rab14 is more broadly distributed within the endosomal system than Rab4 (Yamamoto et al., 2010) and Rab14, but not Rab4A or Rab4B, is a substrate for the isolated GAP domain of AS160 (Mîinea et al., 2005). Rabip4/RUFY1 has been implicated in the sorting of GLUT4 into GSVs in 3T3-L1 adipocytes (Mari et al., 2006) and it has been proposed that Rab14 first recruits Rabip4/RUFY1 to endosomes, which then recruits Rab4 (Yamamoto et al.).

That overexpression of constitutively-active Rab14 and depletion of endogenous Rab14 by shRNA-mediated knockdown both inhibit sorting of GLUT4 out of a compartment(s) characteristic of early endosomes, suggests that an optimal level of Rab14 function is required for normal endosomal sorting to proceed. We propose a model by which by exceeding the optimal amount of Rab14 on the endosomal membrane, the effective exchange of an effector such as Rabip4/RUFY1 between Rab14 and Rab4 is prevented, thus inhibiting GLUT4 transit through this compartment as it matures. By contrast, a reduction in the level of Rab14 could limit the recruitment of Rabip4/RUFY1 to endosomes and thus prevent GLUT4 sorting.

In L6 muscle cells Rab14 overexpression has been reported to increase the size of punctate structures containing a myc-tagged GLUT4 (Ishikura et al., 2007) and we have been able to confirm this observation, albeit to a lesser extent than we see in 3T3-L1 adipocytes (S.E.R., J.M.T., unpublished data). In L6 muscle cells Rab14 knockdown also inhibits insulin-stimulated GLUT4 translocation to the plasma membrane (Ishikura and Klip, 2008) although in 3T3-L1 adipocytes it has been reported to have either no effect (Sano et al., 2008) or a partial inhibition (Chen et al., 2012). The reason for these discrepancies are not known, but a contributing factor could be functional redundancy between Rab4 and Rab14 and the differing degrees to which these proteins contribute to GLUT4 trafficking between different cell lines. Finally, we cannot completely exclude the possibility that Rab14 has an additional role in the trafficking of GLUT4 to the plasma membrane from intracellular compartments; indeed Chen and co-workers have proposed that Rab14 may be involved in the translocation of GLUT4 from an endosomal compartment to the plasma membrane of 3T3-L1 adipocytes (Chen et al., 2012). This proposal was based on the frequent presence of Rab14 on GLUT4 vesicles fusing with the plasma membrane, an observation not replicated in our own experiments (supplementary material Fig. S4). However, the observation that Rab14 acts at an intermediate step in the recycling of transferrin receptor (Linford et al., 2012) appears to be more consistent with Rab14 acting on an intracellular GLUT4 trafficking step rather than direct delivery to the plasma membrane.

Clearly we need a much greater understanding of the trafficking route that GLUT4 takes en route from endosomes to the plasma membrane via the GSV compartment, and the role of Rab14 effectors and how they cycle on and off Rab14 during the various fusion and fission cycles involved, before we can fully appreciate the role of Rab14 in GLUT4 trafficking. However, to conclude, we suggest that in adipocytes the principal role of Rab14 is to control the trafficking of GLUT4 through early endosomes to the TGN, rather than orchestrate its translocation from GSVs directly to the plasma membrane.

## Materials and Methods

### Cells and reagents

The murine 3T3-L1 fibroblast clone was obtained from ATCC (CL-173; Manassas, USA). Antibodies against GLUT4 (1F8) and Rab14 were from Abcam (Cambridge, UK). Anti-TGN38 antibody was a gift from G. Banting (University of Bristol, UK). Anti-HA antibody was from Covance (Berkeley, USA) and rabbit anti-GFP antibody was from Life Technologies (Paisley, UK). Secondary antibodies coupled to fluorophores and foetal bovine serum (FBS) were from Life Technologies. Troglitazone was from Merck Chemicals (Nottingham, UK). Glass bottom culture dishes were from MatTek (Ashland, USA). Unless stated otherwise, all other chemicals, biochemicals and tissue-culture reagents were from Life Technologies, New England Biolabs (Hitchin, UK) or Sigma–Aldrich (Poole, UK). Oligonucleotides were from Eurofins MWG Operon (London, UK).

### Plasmids

The source pGFP-Rab14 WT and Q70L plasmids used in this study are as previously described (Kelly et al. 2009). pmCherry-Rab14 WT was constructed by *Bgl*II and *Bam*HI excision of Rab14 from pGFPRab14WT and ligation into *Bam*HI-digested pmCherry-c1. pmCherry-Rab14S25N was constructed by QuikChange site directed mutagenesis (Stratagene, La Jolla, CA, USA) utilizing sense primer GGAGTAGGAAAAAATTGCTTGCTTCATC and antisense primer GATGAAGCAAGCAATTTTTTCCTACTCC, with pmCherry-Rab14WT as template. The plasmid pmCherry-Rab14Q70L was generated by digesting pEGFP-c1-Rab14Q70L with enzymes *Bgl*II and *Kpn*I, and ligating the fragment encoding Rab14Q70L into pmCherry-c1 digested with the same enzymes. The plasmid encoding TDimer2-IRAP-pHluorin was a gift from T. Xu (Institute of Biophysics, Chinese Academy of Sciences, China). The plasmid encoding IRAP-pHluorin was generated by amplifying IRAP-pHluorin from n1-TDimer2-IRAP-pHlourin by PCR, digesting the PCR product with enzymes NheI and NotI, and ligating this with n1-TDimer2-IRAP-pHluorin digested with the same enzymes. The plasmid encoding HA-GLUT4-mCherry was generated by amplifying mCherry from pmCherry-c1, digesting the PCR product with enzymes *Bam*HI and *Kpn*I, and ligating this with plasmid HA-GLUT4-GFP-pQB125 digested with the same enzymes.

### Cell culture, adipocyte differentiation and electroporation

3T3-L1 fibroblasts were grown and differentiated using a modified protocol from Muretta et al. (Muretta et al., 2008). Briefly, confluent 3T3-L1 fibroblasts in 10-cm tissue-culture dishes were incubated for 3 days in DMEM supplemented with 10% (v/v) FBS, 5 µM troglitazone, 166 nM insulin, 0.25 µM dexamethasone and 0.5 mM isomethylbutylxanthine, and then for a further 3 days in DMEM supplemented with 10% FBS, 5 µM troglitazone, 166 nM insulin. 4–5 days after the start of differentiation, 3T3-L1 adipocytes were electroporated with 45 µg DNA at 180 V and 950 µF, as described previously (Zeigerer et al., 2002), plated on glass bottom culture dishes, and incubated with DMEM supplemented with 10% FBS for 24 hours. Cells were serum starved for 3 hours before stimulation with 87 nM insulin for 30 minutes, as required. Cells were fixed in 4% (w/v) paraformaldehyde.

### Confocal microscopy, immunofluorescence staining, image and statistical analysis

Confocal microscopy of fixed cells was performed on a TCS-SP2-AOBS confocal laser scanning system (Leica, Heidelberg, Germany) attached to a DM IRE2 inverted epifluorescence microscope (Leica) using a 63× oil lens (NA=1.4). GFP was excited at a wavelength of 488 nm and emission wavelengths were collected between 500 and 530 nm; mCherry was excited at a wavelength of 543 nm and emission wavelengths were collected between 580 and 631 nm; Alexa Fluor 633 was excited at a wavelength of 633 nm and emission wavelengths were collected between 642 and 705 nm.

In immunofluorescence staining experiments, fixed 3T3-L1 adipocytes were permeabilised for 5 minutes in 0.1% (w/v) saponin/PBS, blocked for 30 minutes in 1% (w/v) BSA/0.01% saponin/PBS and subsequently incubated for 1 hour in the following antibodies diluted in 1% BSA/0.01% saponin/PBS: anti-GLUT4 (1:200 dilution), anti-Rab14 (1:50 dilution) and anti-TGN38 (1:250 dilution). The cells were washed in PBS and incubated for a further hour in a 1:1000 dilution of goat

anti-mouse or anti-rabbit secondary antibodies coupled to Alexa Fluor 488 or 568 in 1% BSA/0.01% saponin/PBS. The cells were washed and imaged in PBS. To inspect the localisation of internalised GLUT4, cells were electroporated with a plasmid encoding HA-GLUT4. After 24 hours, cells were serum starved, stimulated with insulin, incubated for 30 minutes at 15℃ in serum-free medium supplemented with anti-HA antibody (1:200 dilution), and subsequently incubated for the indicated time at 37℃ in serum-free medium. Cells were fixed, permeabilised, blocked and incubated in a 1:1000 dilution of goat anti-mouse secondary antibody coupled to Alexa Fluor 488 in 1% BSA/0.01% saponin/PBS, as already described. To inspect the localisation of the transferrin receptor, cells were electroporated with a plasmid encoding the human transferrin receptor. After 24 hours, cells were serum starved for 3 hours and incubated for 30 minutes in serum-free medium supplemented with 30 µg/ml transferrin coupled to Alexa Fluor 633, prior to fixation.

Quantification of the number of enlarged vesicular structures with visible lumens was determined by visual inspection. The diameter of enlarged vesicular structures was determined using the line tool in Volocity (PerkinElmer, Coventry, UK). Statistical analysis was performed in Microsoft Excel (Redmond, USA) using a two-tailed Student's *t*-test with a p value of less than 0.05 taken as being significant.

#### Section light electron microscopy

3T3-L1 adipocytes were electroporated with a plasmid encoding GFP-Rab14Q70L and, 24 hours later, were fixed for 2 hours in 2% paraformaldehyde-0.2% glutaraldehyde in 0.1 M phosphate buffer, pH 7.4. Cells were washed, soaked in 1% gelatin in phosphate buffer, detached by scraping and centrifuged for 5 seconds at 13,200 rpm. After washing, cells were embedded in 12% gelatin in phosphate buffer for 10 minutes at 37℃. The solidified gelatin was stored on ice for 30 minutes, cut into small cubes and cryoprotected by infiltration with 2.3 M sucrose in phosphate buffer overnight at 4℃. The cubes were then mounted on aluminium pins and frozen and stored in liquid nitrogen until sectioning. 100 nm-thick, cryosections were cut with an EM UC6 microtome (Leica) equipped with a FC6 Cryo unit (Leica). Sections were collected on droplets of 1% methylcellulose-1.75 M sucrose, and transferred to formvar film-coated, carbon-coated, copper 'finder' grids.

Grid-mounted cells were incubated in PBS for 30 minutes at 37℃, incubated with DAPI to label nuclei, and transferred to 50% glycerol/PBS. Cells expressing GFP-Rab14Q70L were identified using an AM total internal reflection fluorescence multi-colour system (Leica) in widefield mode attached to a DMI 6000 inverted epifluorescence microscope (Leica). Grid-mounted cells were incubated with 100 µM glycine in PBS for 15 minutes at room temperature. Non-specific interactions were blocked by incubation in 0.1% BSA/PBS for 15 minutes at room temperature. Grids were then incubated for 1 hour at room temperature in a 1:25 dilution of rabbit anti-GFP in 0.1% BSA/PBS. After washing in 0.1% BSA/PBS, the grids were incubated for 20 minutes at room temperature in 15 nm protein gold A in 0.1% BSA/PBS. Grids were washed with 0.1% BSA/PBS and distilled water, and counterstained with a solution consisting of 3% uranyl acetate and 2% methylcellulose (1:9 ratio), for 5 minutes on ice. Dried grids were examined on a Tecnai 12 120 kV BioTwin Spirit transmission electron microscope (FEI, Hillsboro, USA) connected to an Eagle CCD camera (FEI).

#### Electron microscopy-based internalisation assay

3T3-L1 adipocytes stably co-expressing HA-GLUT4-GFP and a Rab14 or scrambled shRNA construct were produced as described (Brewer et al., 2011; Sano et al., 2008) and serum starved for 3 hours before stimulation with 87 nM insulin for 20 minutes. Subsequent samples were prepared as described in (Cortese et al., 2008). Briefly, cells were incubated with anti-HA antibody for 20 minutes at 15℃. Unbound antibody was removed by extensive washing in ice cold PBS, before incubating cells in rabbit anti-mouse bridging antibody for a further 20 minutes at 15℃. Cells were washed with ice cold PBS and incubated with 5 nm Protein A gold. Finally, cells were warmed to 37℃ and allowed to internalise the antibody–gold complex for various time points before fixing in 2% paraformaldehyde–0.2% glutaraldehyde. The cells were then processed for section light electron microscopy as described above. In addition to incubations in DAPI, grid-mounted cells were also labelled with goat anti-mouse Alexa Fluor 633 before imaging in widefield mode on a TIRF microscope (inverted Leica DMI 6000).

Whole cells were imaged by transmission electron microscopy and gold labelling was quantified by counting all gold particles located within 30 nm (Klumperman et al., 1998) of the following compartments: (i) plasma membrane (PM); (ii) clathrin-coated pits/vesicles at the PM (vesicles with an electron dense coat attached to the PM); (iii) vesicles/tubules near the PM (clear vesicular tubular elements, less than 200 nm in diameter, within 200 nm of the plasma membrane); (iv) early endosomes greater than 200 nm in diameter with 4 or less intra-lumenal vesicles (ILVs); (v) early endosomes greater than 200 nm in diameter with 5–8 ILVs; (vi) late endosomes (vacuoles greater than 200 nm with more than 8 ILVs); (vii) lysosomes (electron dense compartments, greater than 200 nm in diameter with or without internal vesicles or lamellar membranes); (viii) Golgi (a stack of 3 or more cisternae); (ix) TGN (vesicular and tubular strictures within 400 nm of the Golgi stack); (x) clusters of 50–100 nm diameter vesicles (8 or more) located within the perinuclear region of the cell; and (xi) vesicular tubular elements in the perinuclear region (vesicular tubular profiles within 400 nm of the nucleus) (supplementary material Fig. S2). Gold counts were expressed as the percentage of total gold within each and normalised to total membrane length for each organelle (µm). Statistical analysis was performed in SPSS Statistics (New York, USA) using a Kruskal–Wallis ANOVA test with p values of less than 0.05 or 0.01 taken as being significant.

#### GLUT4 translocation assay

The insulin-stimulated redistribution of GLUT4 to the plasma membrane was examined using the HA-GLUT4-GFP fusion protein, using a modified method from Welsh et al. (Welsh et al., 2007). Adipocytes were electroporated with plasmids encoding HA-GLUT4-GFP and mCherry alone or mCherry-Rab14Q70L. 24 hours after electroporation, cells were serum starved, stimulated with insulin, as required, and fixed, as already described. The appearance of the HA epitope was detected in non-permeabilised cells by staining with anti-HA antibody (1:500) followed by incubation with Alexa Fluor 633 goat anti-mouse IgG (1:1000), and cells were imaged by confocal microscopy. Cells expressing the HA-GLUT4-GFP and mCherry alone or mCherry-Rab14Q70L constructs were identified, and images were captured for both the 633 nm and GFP channels. Approximately 20 cells per condition were imaged in each experiment. Unlike for GFP, only HA fluorescence at the cell surface was considered to minimise cross-talk between mCherry (fused to the co-expressed Rab) and 633 (HA) channels. The cell surface was delineated by drawing a region of interest around it and then the mean 633 nm intensity within this region, and the mean GFP intensity throughout the whole cell were measured using Metamorph (Molecular Devices, West Chester, USA). Each cell was corrected for background by subtracting the mean 633 nm and GFP fluorescence in non-expressing cells. To determine the surface-to-total distribution of GLUT4, that is the relative amount of GLUT4 incorporated into the plasma membrane, the 633:GFP ratio was calculated for each cell to normalise the expression level of the HA-GLUT4-GFP construct, and the mean 633:GFP ratio was determined for each condition. In each experiment, mean 633:GFP ratios were normalised so that the mean 633:GFP ratio in mCherry alone expressing insulin-stimulated cells was equal to 1. Overexpression of the Rab14 constructs had no affect on the total level of expression of GLUT4-GFP (data not shown).

#### TIRF microscopy

TIRF microscopy of live cells was performed at 37℃ on a AM TIRF multi-colour system (Leica) attached to a DMI 6000 inverted epifluorescence microscope (Leica) using a 100× oil lens (NA=1.46). Images were captured using an EM-CCD camera (Hamamatsu, Japan) between approx. 2–3 fps at a penetration depth of 90 nm. pHluorin was excited at a wavelength of 488 nm and emission wavelengths were collected between 507 and 543 nm; mCherry was excited at a wavelength of 561 nm and emission wavelengths were collected between 584 and 616 nm. When required, cells were treated with 87 nM insulin on the microscope using a home-made perfusion system.

## Acknowledgements

We are grateful to Mary McCaffrey (University College Cork, Ireland) and Tao Xu (Institute of Biophysics, Chinese Academy of Sciences, China) for gifts of the Rab14 and TDimer2-IRAP-pHluorin plasmids, respectively and to Gus Lienhard (Dartmouth College) for the lentiviral Rab14 shRNA construct. We also thank George Banting (University of Bristol, UK) for providing the anti-TGN38 antibody, and Fred Boal (University of Bristol, UK) for useful discussions.

## Author contributions

S.E.E., L.R.H., C.C.M., E.E.K., M.W.M., P.V. and J.M.T. conceived and designed experiments. S.E.E., L.R.H., S.S., E.E.K. and C.C.M. performed experiments. S.E.E., L.R.H., S.S., M.T.M., C.C.M., P.V. and J.M.T. analysed the data. S.E.E., L.R.H., M.T.M., M.W.M., C.C.M., P.V. and J.M.T. wrote and reviewed the manuscript.

## Funding

We thank the Biotechnology and Biological Sciences Research Council (BBSRC) and (OSI) Prosidion for supporting S.E.R. and the Medical Research Council [grant number G0900177] for supporting L.H. We also thank DiabetesUK for a grant to J.M.T. that supported part of this work and Science Foundation Ireland (SFI) for an

Investigator Grant [09/IN.1/B2629] to M.M.C. Deposited in PMC for release after 6 months.

Supplementary material available online at
http://jcs.biologists.org/lookup/suppl/doi:10.1242/jcs.104307/-/DC1

## References


**Antonescu, C. N., Díaz, M., Femia, G., Planas, J. V. and Klip, A.** (2008). Clathrin-dependent and independent endocytosis of glucose transporter 4 (GLUT4) in myoblasts: regulation by mitochondrial uncoupling. *Traffic* **9**, 1173-1190.

**Brewer, P. D., Romenskaia, I., Kanow, M. A. and Mastick, C. C.** (2011). Loss of AS160 Akt substrate causes Glut4 protein to accumulate in compartments that are primed for fusion in basal adipocytes. *J. Biol. Chem.* **286**, 26287-26297.

**Bucci, C., Parton, R. G., Mather, I. H., Stunnenberg, H., Simons, K., Hoflack, B. and Zerial, M.** (1992). The small GTPase rab5 functions as a regulatory factor in the early endocytic pathway. *Cell* **70**, 715-728.

**Chen, Y., Wang, Y., Zhang, J., Deng, Y., Jiang, L., Song, E., Wu, X. S., Hammer, J. A., Xu, T. and Lippincott-Schwartz, J.** (2012). Rab10 and myosin-Va mediate insulin-stimulated GLUT4 storage vesicle translocation in adipocytes. *J. Cell Biol.* **198**, 545-560.

**Cormont, M., Bortoluzzi, M. N., Gautier, N., Mari, M., van Obberghen, E. and Le Marchand-Brustel, Y.** (1996). Potential role of Rab4 in the regulation of subcellular localization of Glut4 in adipocytes. *Mol. Cell. Biol.* **16**, 6879-6886.

**Cortese, K., Sahores, M., Madsen, C. D., Tacchetti, C. and Blasi, F.** (2008). Clathrin and LRP-1-independent constitutive endocytosis and recycling of uPAR. *PLoS ONE* **3**, e3730.

**Eguez, L., Lee, A., Chavez, J. A., Miinea, C. P., Kane, S., Lienhard, G. E. and McGraw, T. E.** (2005). Full intracellular retention of GLUT4 requires AS160 Rab GTPase activating protein. *Cell Metab.* **2**, 263-272.

**Harris, E. and Cardelli, J.** (2002). RabD, a Dictyostelium Rab14-related GTPase, regulates phagocytosis and homotypic phagosome and lysosome fusion. *J. Cell Sci.* **115**, 3703-3713.

**Huang, S. and Czech, M. P.** (2007). The GLUT4 glucose transporter. *Cell Metab.* **5**, 237-252.

**Ishikura, S. and Klip, A.** (2008). Muscle cells engage Rab8A and myosin Vb in insulin-dependent GLUT4 translocation. *Am. J. Physiol. Cell Physiol.* **295**, C1016-C1025.

**Ishikura, S., Bilan, P. J. and Klip, A.** (2007). Rabs 8A and 14 are targets of the insulin-regulated Rab-GAP AS160 regulating GLUT4 traffic in muscle cells. *Biochem. Biophys. Res. Commun.* **353**, 1074-1079.

**Ishikura, S., Koshkina, A. and Klip, A.** (2008). Small G proteins in insulin action: Rab and Rho families at the crossroads of signal transduction and GLUT4 vesicle traffic. *Acta Physiol. (Oxf.)* **192**, 61-74.

**Jiang, L., Fan, J., Bai, L., Wang, Y., Chen, Y., Yang, L., Chen, L. and Xu, T.** (2008). Direct quantification of fusion rate reveals a distal role for AS160 in insulin-stimulated fusion of GLUT4 storage vesicles. *J. Biol. Chem.* **283**, 8508-8516.

**Junutula, J. R., De Maziére, A. M., Peden, A. A., Ervin, K. E., Advani, R. J., van Dijk, S. M., Klumperman, J. and Scheller, R. H.** (2004). Rab14 is involved in membrane trafficking between the Golgi complex and endosomes. *Mol. Biol. Cell* **15**, 2218-2229.

**Kaddai, V., Le Marchand-Brustel, Y. and Cormont, M.** (2008). Rab proteins in endocytosis and Glut4 trafficking. *Acta Physiol. (Oxf.)* **192**, 75-88.

**Kane, S., Sano, H., Liu, S. C., Asara, J. M., Lane, W. S., Garner, C. C. and Lienhard, G. E.** (2002). A method to identify serine kinase substrates. Akt phosphorylates a novel adipocyte protein with a Rab GTPase-activating protein (GAP) domain. *J. Biol. Chem.* **277**, 22115-22118.

**Karylowski, O., Zeigerer, A., Cohen, A. and McGraw, T. E.** (2004). GLUT4 is retained by an intracellular cycle of vesicle formation and fusion with endosomes. *Mol. Biol. Cell* **15**, 870-882.

**Kelly, E. E., Horgan, C. P., Adams, C., Patzer, T. M., Ní Shúilleabháin, D. M., Norman, J. C. and McCaffrey, M. W.** (2009). Class I Rab11-family interacting proteins are binding targets for the Rab14 GTPase. *Biol Cell.* **102**, 52-62.

**Kessler, A., Tomas, E., Immler, D., Meyer, H. E., Zorzano, A. and Eckel, J.** (2000). Rab11 is associated with GLUT4-containing vesicles and redistributes in response to insulin. *Diabetologia* **43**, 1518-1527.

**Klumperman, J., Kuliawat, R., Griffith, J. M., Geuze, H. J. and Arvan, P.** (1998). Mannose 6-phosphate receptors are sorted from immature secretory granules via adaptor protein AP-1, clathrin, and syntaxin 6-positive vesicles. *J. Cell Biol.* **141**, 359-371.

**Kyei, G. B., Vergne, I., Chua, J., Roberts, E., Harris, J., Junutula, J. R. and Deretic, V.** (2006). Rab14 is critical for maintenance of Mycobacterium tuberculosis phagosome maturation arrest. *EMBO J.* **25**, 5250-5259.

**Larance, M., Ramm, G., Stöckli, J., van Dam, E. M., Winata, S., Wasinger, V., Simpson, F., Graham, M., Junutula, J. R., Guilhaus, M. et al.** (2005). Characterization of the role of the Rab GTPase-activating protein AS160 in insulin-regulated GLUT4 trafficking. *J. Biol. Chem.* **280**, 37803-37813.

**Larance, M., Ramm, G. and James, D. E.** (2008). The GLUT4 code. *Mol. Endocrinol.* **22**, 226-233.

**Leney, S. E. and Tavaré, J. M.** (2009). The molecular basis of insulin-stimulated glucose uptake: signalling, trafficking and potential drug targets. *J. Endocrinol.* **203**, 1-18.

**Linford, A., Yoshimura, S., Nunes Bastos, R., Langemeyer, L., Gerondopoulos, A., Rigden, D. J. and Barr, F. A.** (2012). Rab14 and its exchange factor FAM116 link endocytic recycling and adherens junction stability in migrating cells. *Dev. Cell* **22**, 952-966.

**Lodhi, I. J., Chiang, S. H., Chang, L., Vollenweider, D., Watson, R. T., Inoue, M., Pessin, J. E. and Saltiel, A. R.** (2007). Gapex-5, a Rab31 guanine nucleotide exchange factor that regulates Glut4 trafficking in adipocytes. *Cell Metab.* **5**, 59-72.

**Mari, M., Monzo, P., Kaddai, V., Keslair, F., Gonzalez, T., Le Marchand-Brustel, Y. and Cormont, M.** (2006). The Rab4 effector Rabip4 plays a role in the endocytotic trafficking of Glut 4 in 3T3-L1 adipocytes. *J. Cell Sci.* **119**, 1297-1306.

**Martin, S., Ramm, G., Lyttle, C. T., Meerloo, T., Stoorvogel, W. and James, D. E.** (2000). Biogenesis of insulin-responsive GLUT4 vesicles is independent of brefeldin A-sensitive trafficking. *Traffic* **1**, 652-660.

**Mîinea, C. P., Sano, H., Kane, S., Sano, E., Fukuda, M., Peränen, J., Lane, W. S. and Lienhard, G. E.** (2005). AS160, the Akt substrate regulating GLUT4 translocation, has a functional Rab GTPase-activating protein domain. *Biochem. J.* **391**, 87-93.

**Muretta, J. M., Romenskaia, I. and Mastick, C. C.** (2008). Insulin releases Glut4 from static storage compartments into cycling endosomes and increases the rate constant for Glut4 exocytosis. *J. Biol. Chem.* **283**, 311-323.

**Pereira-Leal, J. B. and Seabra, M. C.** (2000). The mammalian Rab family of small GTPases: definition of family and subfamily sequence motifs suggests a mechanism for functional specificity in the Ras superfamily. *J. Mol. Biol.* **301**, 1077-1087.

**Proikas-Cezanne, T., Gaugel, A., Frickey, T. and Nordheim, A.** (2006). Rab14 is part of the early endosomal clathrin-coated TGN microdomain. *FEBS Lett.* **580**, 5241-5246.

**Ross, S. A., Scott, H. M., Morris, N. J., Leung, W. Y., Mao, F., Lienhard, G. E. and Keller, S. R.** (1996). Characterization of the insulin-regulated membrane amino-peptidase in 3T3-L1 adipocytes. *J. Biol. Chem.* **271**, 3328-3332.

**Ross, S. A., Herbst, J. J., Keller, S. R. and Lienhard, G. E.** (1997). Trafficking kinetics of the insulin-regulated membrane aminopeptidase in 3T3-L1 adipocytes. *Biochem. Biophys. Res. Commun.* **239**, 247-251.

**Sakamoto, K. and Holman, G. D.** (2008). Emerging role for AS160/TBC1D4 and TBC1D1 in the regulation of GLUT4 traffic. *Am. J. Physiol. Endocrinol. Metab.* **295**, E29-E37.

**Sano, H., Kane, S., Sano, E., Mîinea, C. P., Asara, J. M., Lane, W. S., Garner, C. W. and Lienhard, G. E.** (2003). Insulin-stimulated phosphorylation of a Rab GTPase-activating protein regulates GLUT4 translocation. *J. Biol. Chem.* **278**, 14599-14602.

**Sano, H., Eguez, L., Teruel, M. N., Fukuda, M., Chuang, T. D., Chavez, J. A., Lienhard, G. E. and McGraw, T. E.** (2007). Rab10, a target of the AS160 Rab GAP, is required for insulin-stimulated translocation of GLUT4 to the adipocyte plasma membrane. *Cell Metab.* **5**, 293-303.

**Sano, H., Roach, W. G., Peck, G. R., Fukuda, M. and Lienhard, G. E.** (2008). Rab10 in insulin-stimulated GLUT4 translocation. *Biochem. J.* **411**, 89-95.

**Schwenk, R. W., Luiken, J. J. and Eckel, J.** (2007). FIP2 and Rip11 specify Rab11a-mediated cellular distribution of GLUT4 and FAT/CD36 in H9c2-hIR cells. *Biochem. Biophys. Res. Commun.* **363**, 119-125.

**Shewan, A. M., van Dam, E. M., Martin, S., Luen, T. B., Hong, W., Bryant, N. J. and James, D. E.** (2003). GLUT4 recycles via a trans-Golgi network (TGN) subdomain enriched in Syntaxins 6 and 16 but not TGN38: involvement of an acidic targeting motif. *Mol. Biol. Cell* **14**, 973-986.

**Slot, J. W., Geuze, H. J., Gigengack, S., James, D. E. and Lienhard, G. E.** (1991a). Translocation of the glucose transporter GLUT4 in cardiac myocytes of the rat. *Proc. Natl. Acad. Sci. USA* **88**, 7815-7819.

**Slot, J. W., Geuze, H. J., Gigengack, S., Lienhard, G. E. and James, D. E.** (1991b). Immuno-localization of the insulin regulatable glucose transporter in brown adipose tissue of the rat. *J. Cell Biol.* **113**, 123-135.

**Stenmark, H., Parton, R. G., Steele-Mortimer, O., Lütcke, A., Gruenberg, J. and Zerial, M.** (1994). Inhibition of rab5 GTPase activity stimulates membrane fusion in endocytosis. *EMBO J.* **13**, 1287-1296.

**Stöckli, J., Davey, J. R., Hohnen-Behrens, C., Xu, A., James, D. E. and Ramm, G.** (2008). Regulation of glucose transporter 4 translocation by the Rab guanosine triphosphatase-activating protein AS160/TBC1D4: role of phosphorylation and membrane association. *Mol. Endocrinol.* **22**, 2703-2715.

**Sun, Y., Bilan, P. J., Liu, Z. and Klip, A.** (2010). Rab8A and Rab13 are activated by insulin and regulate GLUT4 translocation in muscle cells. *Proc. Natl. Acad. Sci. USA* **107**, 19909-19914.

**Uhlig, M., Passlack, W. and Eckel, J.** (2005). Functional role of Rab11 in GLUT4 trafficking in cardiomyocytes. *Mol. Cell. Endocrinol.* **235**, 1-9.

**Welsh, G. I., Hers, I., Berwick, D. C., Dell, G., Wherlock, M., Birkin, R., Leney, S. and Tavaré, J. M.** (2005). Role of protein kinase B in insulin-regulated glucose uptake. *Biochem. Soc. Trans.* **33**, 346-349.

**Welsh, G. I., Leney, S. E., Lloyd-Lewis, B., Wherlock, M., Lindsay, A. J., McCaffrey, M. W. and Tavaré, J. M.** (2007). Rip11 is a Rab11- and AS160-RabGAP-binding protein required for insulin-stimulated glucose uptake in adipocytes. *J. Cell Sci.* **120**, 4197-4208.

**Yamamoto, H., Koga, H., Katoh, Y., Takahashi, S., Nakayama, K. and Shin, H. W.** (2010). Functional cross-talk between Rab14 and Rab4 through a dual effector, RUFY1/Rabip4. *Mol. Biol. Cell* **21**, 2746-2755.

**Zeigerer, A., Lampson, M. A., Karylowski, O., Sabatini, D. D., Adesnik, M., Ren, M. and McGraw, T. E.** (2002). GLUT4 retention in adipocytes requires two intracellular insulin-regulated transport steps. *Mol. Biol. Cell* **13**, 2421-2435.

**Zerial, M. and McBride, H.** (2001). Rab proteins as membrane organizers. *Nat. Rev. Mol. Cell Biol.* **2**, 107-117.